

## 6. NEUTRON ACTIVATION ANALYSIS OF THE BLOEDKOPPIE AND GAWIB GRANITES AND THE ROCKS OF THE TINKAS FORMATION

Non-destructive neutron activation analysis (NAA) has been applied to the analysis of a diverse range of rock types with great success. Turkstra et al (1971) and Rasmussen (1973) discuss the methods and techniques applicable to this type of analysis. Certain elements are not easily measured using NAA either due to their nuclear properties or the overwhelming presence of a specific interfering activity. For elements of lower concentration and those with interfering isotopes, a greater sensitivity may be achieved from post-irradiation radiochemical separations (Morrison et al, 1969). In this work only the non-destructive method was used for the analysis of the long-lived isotopes of trace elements in the granites and for the short-lived isotope of vanadium in the Tinkas Formation. The nuclear properties of the radio-nuclides and the energies of the photopeaks used in the determination are given in Tables 8 and 10.

Of the elements analyzed, there were no interfering nuclear reactions - neither (n,p) nor (n, $\alpha$ ) from fast neutrons. The type of reactions that could occur were summarized by Turkstra et al (1971, p. 116).

### 8.1 Experimental Procedure

A standard solution containing the elements listed in Table 10, and including lanthanum, thorium, cerium, hafnium and

CONFIDENTIAL

126

europium from Table 8 (with the exception of aluminium, vanadium and dysprosium) was prepared. Approximately 0,25 g were accurately weighed into quartz ampoules, dried under infra-red lamps and sealed. About 0,2 g of each sample was weighed out, sealed in the same manner and irradiated for six hours in the C-position of the poolside rack irradiation facility of SAFARI-1. The neutron flux for this region of the reactor is about  $3 \times 10^{18} \text{ n m}^{-2} \text{ s}^{-1}$  at 20 MW with a cadmium ratio of 60 for  $^{60}\text{Co}$  (1 333 keV) which is a measure of the epithermal flux contribution to the total neutron flux. The higher the cadmium ratio, the lower the epithermal flux. Therefore, due to the presence of uranium the C-position was used in order to minimize the possibility of the formation of interfering activities from fission products.

Counting was done on the system available, a  $50 \text{ cm}^3$  Ge(Li) coaxial detector coupled to a Canberra preamplifier. Output pulses were amplified by a Canberra amplifier, after which the spectral analysis was done using an Intertechnique 4 000 multichannel analyzer. Data were accumulated on magnetic tape using an Ampex TMZ, start-stop tape recorder. Thereafter the data were processed using Yule's (1968) smoothed first derivative method, as modified by Brits (1975) to calculate the integrated peak areas for the spectrum. The resolution for the system is 3 keV for the 1 333 keV  $^{60}\text{Co}$  peak and has a calibration of 0,55 keV/channel. The samples were counted for 30 minutes after a decay of nine days for the elements lanthanum, barium, lutetium and samarium, and 37 days for the elements europium, cobalt, tantalum, rubidium, scandium, terbium, cesium, hafnium, protactinium and cerium.

CONFIDENTIAL

CONFIDENTIAL  
CONFIDENTIAL126  
127

TABLE 10: NUCLEAR DATA FOR RADIONUCLIDES PRODUCED BY THERMAL NEUTRONS

Element	Target Isotope	Isotopic Abundance (%)	Thermal Neutrons Activation Cross-Section <sup>1</sup> (Barn)	Product Isotope	Half-life <sup>2</sup>	γ-Ray Photo-peak measured <sup>3</sup> (keV)
Al	<sup>27</sup> Al	100	0,24	<sup>28</sup> Al	2,31 m	1 779
V	<sup>51</sup> V	99,8	4,9	<sup>52</sup> V	3,76 m	1 434
Dy	<sup>164</sup> Dy	28,2	2 200	<sup>165</sup> Dy	2,32 h	95
Sm	<sup>152</sup> Sm	26,7	210	<sup>153</sup> Sm	47 h	103
Lu	<sup>176</sup> Lu	2,6	2 100	<sup>177</sup> Lu	6,7 d	208
Ba	<sup>130</sup> Ba	0,1	11	<sup>131</sup> Ba	12 d	496
Rb	<sup>85</sup> Rb	72,2	0,7	<sup>86</sup> Rb	18,7 d	1 077
Tb	<sup>159</sup> Tb	100	22	<sup>160</sup> Tb	72,1 d	879
Sc	<sup>45</sup> Sc	100	13	<sup>46</sup> Sc	83,9 d	889
Ta	<sup>181</sup> Ta	100	21	<sup>182</sup> Ta	115 d	1 222
Cs	<sup>133</sup> Cs	100	29	<sup>134</sup> Cs	2,05 y	796
Co	<sup>59</sup> Co	100	17	<sup>60</sup> Co	526 y	1 173
Zn	<sup>64</sup> Zn	48,9	0,47	<sup>65</sup> Zn	245 d	1 115

<sup>1</sup> Chart of the Nuclides<sup>2</sup> Lederer et al (1968)<sup>3</sup> Adams and Dams (1969)

CONFIDENTIAL

CONFIDENTIAL

Spectra derived from Bloedkoppie Granite are shown in Figs. 29 and 30 for the two counting periods, respectively.

All the photopeaks used for the analysis of the elements in Tables 8 and 10 are essentially free from interfering peaks of other isotopes, with the exception of  $^{141}\text{Ce}$  and  $^{153}\text{Sm}$ .  $^{141}\text{Ce}$  has a small interference peak from  $^{59}\text{Fe}$  at 145 keV, and  $^{153}\text{Sm}$  has an interference from the 100 per cent relative intensity  $^{239}\text{Np}$  peak at 103 keV. Removal of these interferences was done by obtaining a pure spectrum of both  $^{59}\text{Fe}$  and  $^{239}\text{Np}$ , from which the relative peak intensities of the various lines could be calculated.  $^{46}\text{Sc}$  (889 keV) has an interference from  $^{110\text{m}}\text{Ag}$  (885 keV), but as silver was not detected, it was discounted.

Approximately 0,2 g of sample from the schists and granofelses of the Tinkas Formation were accurately weighed into polythene capsules. Irradiations were carried out in the pneumatic facility of SAFAFI-1, which has a thermal neutron flux of about  $2,9 \times 10^{18} \text{ n m}^{-2} \text{ s}^{-1}$  at 20 MW, and a cadmium ratio of 33. Samples were irradiated for 20 seconds, allowed to cool for three minutes, and counted for five minutes.

The greatest problem concerning the analysis of vanadium is the high concentration of aluminium. Both  $^{28}\text{Al}$  and  $^{52}\text{V}$  have very short half-lives, and therefore vanadium has to be counted in its presence. In Fig. 31 the  $^{52}\text{V}$  peak lies almost on top of the  $^{28}\text{Al}$  Compton edge, thereby reducing its sensitivity and consequently the detection limit.

CONFIDENTIAL

129

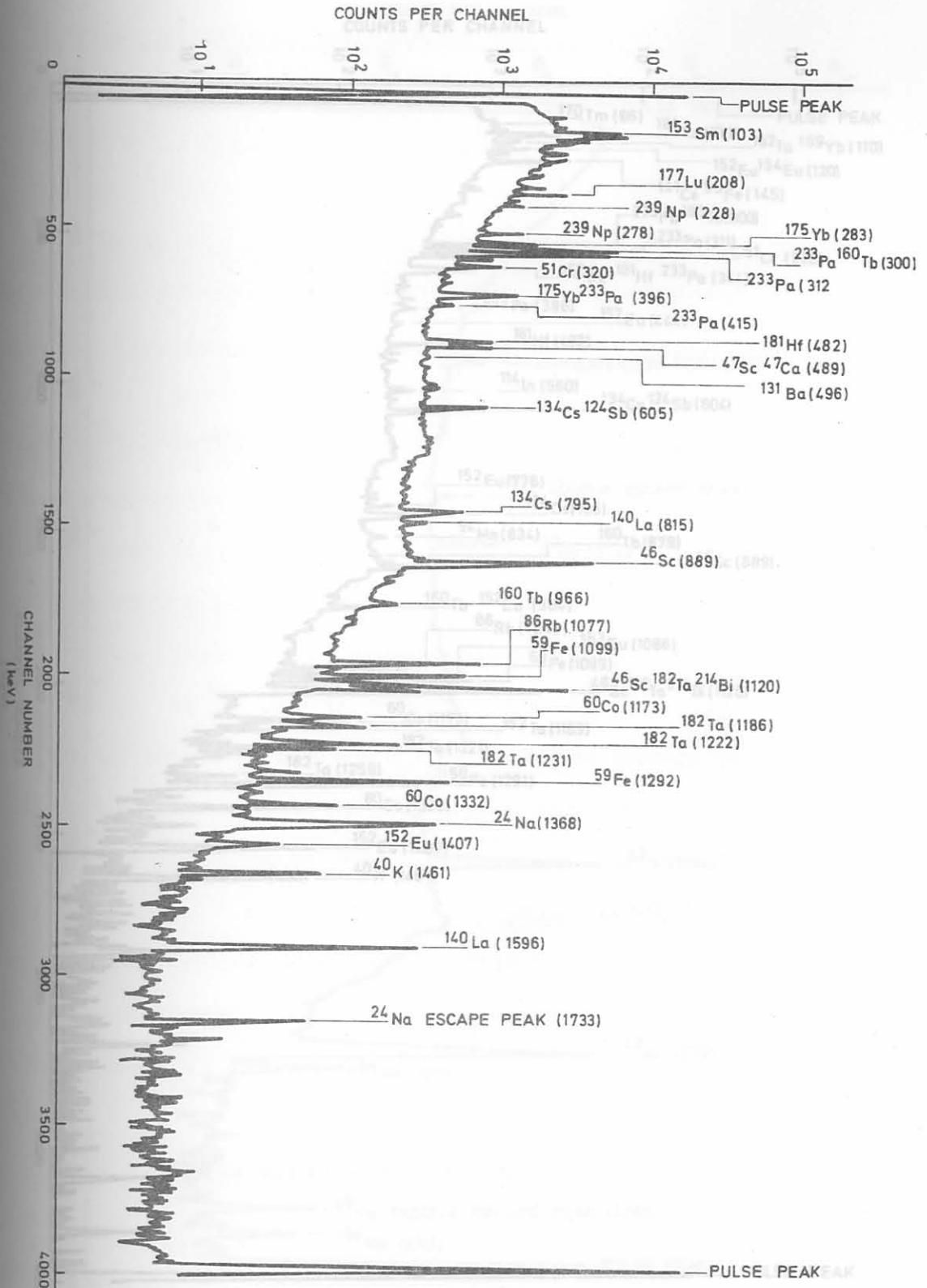


Fig. 29: Gamma-ray spectrum after a decay of nine days for the analysis of lanthanum, barium, lutetium and samarium in the Bloedkoppie Granite.   
 cerium, protactinium (thorium) and cerium in the Bloedkoppie Granite.

CONFIDENTIAL

CONFIDENTIAL

130

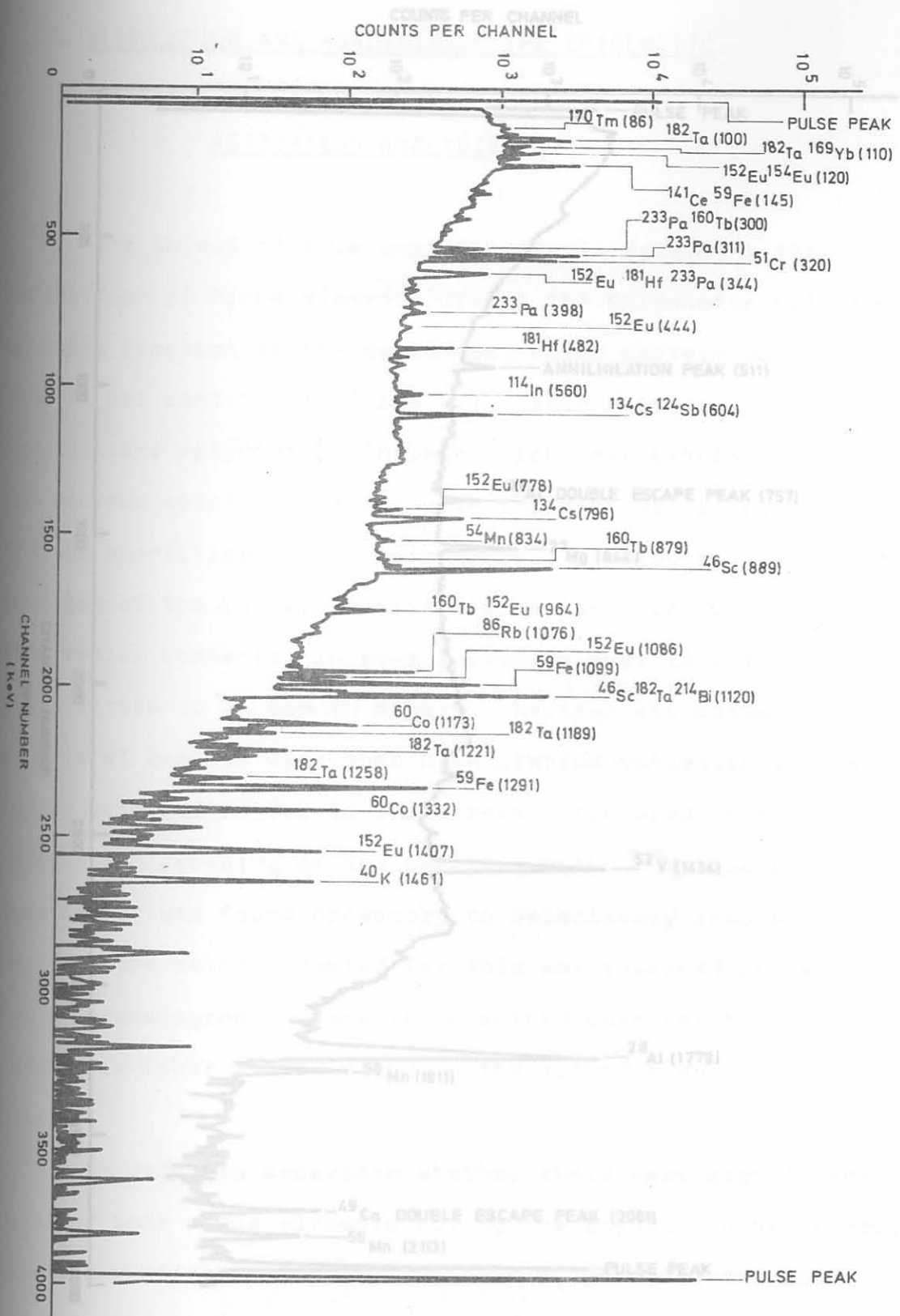


Fig. 30: Gamma-ray spectrum after a decay of 37 days for the analysis of europium, cobalt, tantalum, rubidium, samarium, terbium, cesium, hafnium, protactinium (thorium) and cerium in the Bloedkoppie Granite.

CONFIDENTIAL

CONFIDENTIAL

131

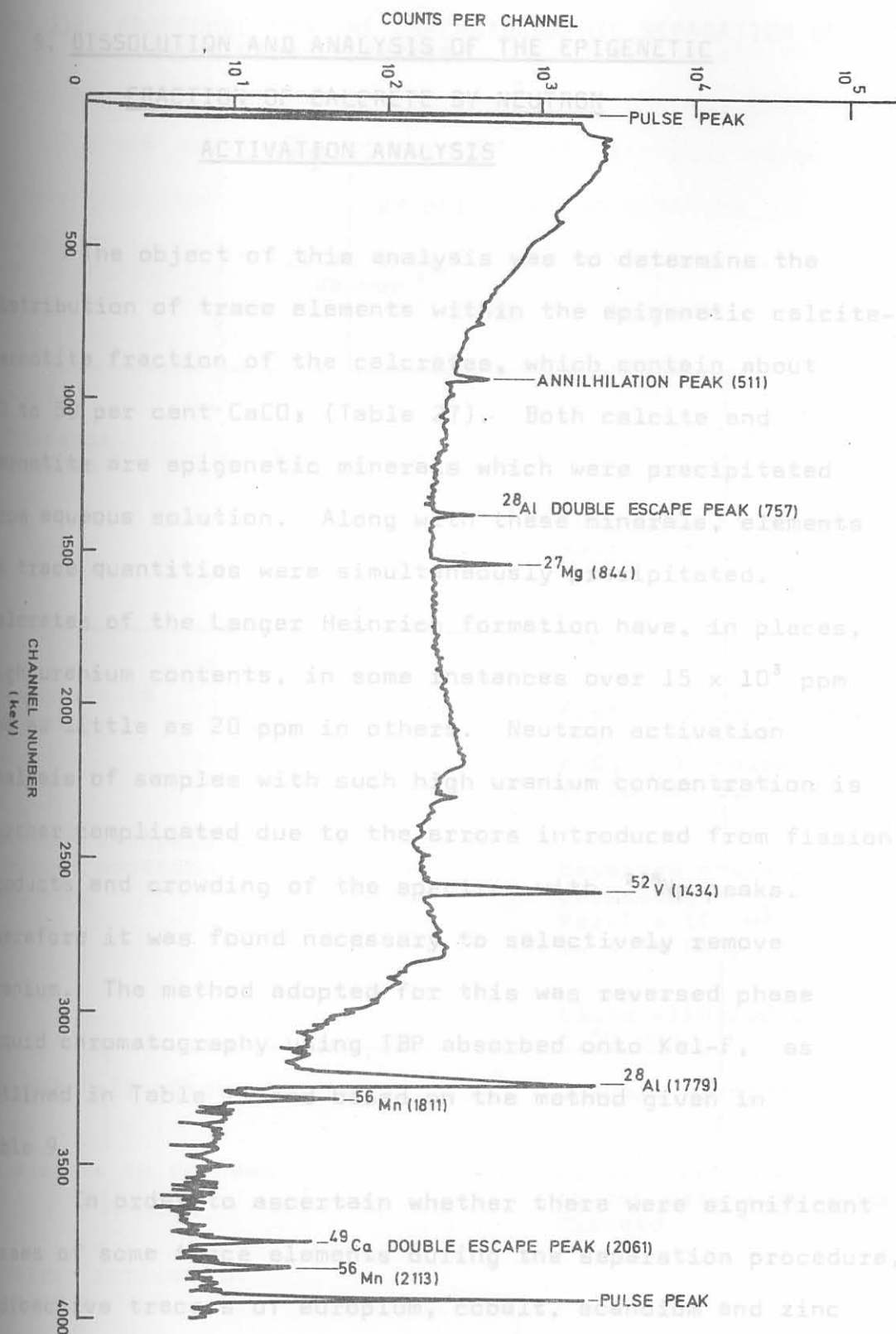


Fig. 31: Gamma-ray spectrum for the analysis of vanadium in the schists and granofelses of the Tinkas Formation.

CONFIDENTIAL